STScI | SPACE TELESCOPE SCIENCE INSTITUTE

Instrument Science Report ACS 2022-07

Fading Hot Pixels in ACS/WFC

J. E. Ryon, N. A. Grogin, M. C. McDonald

December 13, 2022

Abstract

In this report, we study hot pixels that do not accumulate dark current at a constant rate over the course of an exposure in the ACS/WFC detectors. The dark rate drops with time in many of these hot pixels, i.e., they fade during an exposure. We also find that the degree of fading is correlated with dark rate itself, and that there is no obvious evolution in the degree of fading over the lifetime of ACS. Very hot pixels are least likely to be properly dark-corrected with CALACS, so we now flag pixels $\geq$20 e^-/s as unusable for science purposes in the WFC dark reference files and data quality arrays of science products.

1 Introduction

The low-Earth orbit radiation environment of the Hubble Space Telescope (HST) damages the Advanced Camera for Surveys (ACS) Wide Field Channel (WFC) charge-coupled device (CCD) detectors. The type of damage that most degrades the CCDs' performance is called displacement damage. It is largely caused by protons trapped in Earth's radiation belts interacting with silicon atoms in the detectors. The silicon atoms are displaced from their positions in the silicon lattice, giving rise to vacancies. Vacancies can pair up with impurity atoms or other vacancies to create defects in the lattice, a small fraction of which become permanent (Jones, 2000). Defects create new energy levels in the silicon bandgap, resulting in charge trapping and charge generation, which cause charge transfer efficiency (CTE) losses and increased dark current, respectively (Janesick, 2001).

In regions of high electric field, charge generation in lattice defects can be greatly enhanced, called field-assisted charge generation (Janesick, 2001; Sirianni et al., 2006). This

gives rise to individual pixels with anomalously high dark currents, called warm and hot pixels. Electric fields in a pixel are strongest at the beginning of an exposure, and weaken as charge is accumulated. Field-assisted charge generation is therefore expected to decrease as the charge in a pixel grows during an exposure, resulting in dark rates that decrease as a function of exposure time (Janesick, 2001). This effect has never been characterized for hot pixels in the WFC detectors.

Warm and hot pixels have been growing in number since the installation of ACS on HST in 2002 (Ryon et al., 2022). Pixels are flagged as warm or hot if they have dark rates of 0.06-0.14 e^-/s/pixel or >0.14 e^-/s/pixel in the dark reference files, respectively (Desjardins et al., 2018; Ogaz et al., 2015). The WFC CCDs are annealed about once per month, which involves heating the detectors from -81°C to +20°C. Anneals temporarily reduce the numbers of warm and hot pixels, slowing the overall growth rate, but do not repair all of them (McDonald et al., 2020).

The CCD Daily Monitor program (recent program ID: 16970) obtains four 1000.5s dark frames three times each week to monitor the dark current behavior of WFC. Darks obtained between subsequent anneals are combined into dark reference files, also called superdarks, which provide the typical dark rate in each pixel. The global dark current and warm/hot pixels are removed from a science frame by scaling the superdark by the exposure time of the science frame and subtracting the inferred dark current signal from the science frame, pixel-by-pixel. For this dark correction technique to remove all dark current signal from the frame, each pixel's dark rate must be constant with exposure time. Some pixels are known to have dark rates that fluctuate on timescales of hours or days with the appearance of random telegraph signal (RTS) noise (Ryon et al., 2022). These "unstable" pixels, which were characterized by Borncamp et al. (2017), are flagged as unusable in the WFC images' data quality (DQ) arrays.

Recently, a pilot program to test the efficacy of short-exposure calibration dark frames led us to recognize that the dark rates of many "stable" hot pixels were significantly higher than in the superdark. In other words, these "stable" hot pixels appeared to "fade" substantially with exposure time, warranting further investigation. In Section 2, we describe the identification of hot pixels with mismatched dark rates. We discuss further analysis of fading behavior of individual pixels in Section 3 and study the evolution of fading hot pixels over the lifetime of ACS in Section 4. Effects on science data and our approach to addressing the poor correction of fading hot pixels are described in Section 5. We discuss the physical underpinnings of fading hot pixels and conclude this report in Section 6.

2 Identifying Fading Hot Pixels

In October 2020, the calibration program 16419 obtained a set of dark frames with about half of the exposure time (550s) and LED post-flash illumination (22 e^-) as the dark frames obtained by the CCD Daily Monitor program (1000s, 55 e^-). This program, which we call the Pilot program, obtained twice as many darks as the Daily Monitor program, but over the same period of time and at the same cadence. The main purpose of the Pilot program was to determine whether dark reference files made from shorter darks with lower backgrounds would improve dark correction of external frames, as discussed in Ryon et al. (2021).

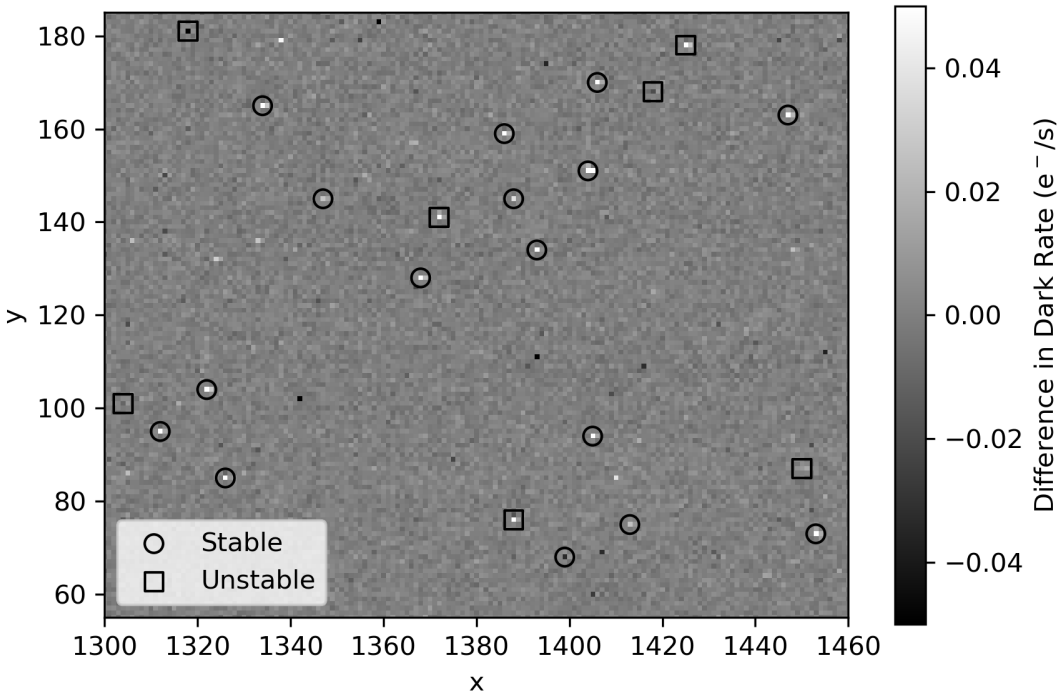

Figure 1: Difference image of Daily Monitor CTE-corrected superdark (DKC) subtracted from its pilot counterpart. The 160×130 pixel section shown is on amplifier C, near the serial register. Circles mark stable pixels and squares mark unstable pixels (DQ flag 32), both >5 e^-/s.

Superdarks were created from each program's dark frames with the reference file pipeline (Desjardins et al., 2018). To visually compare the differences in dark rate between the two datasets, we subtracted the Daily Monitor CTE-corrected superdark (DKC) from its Pilot counterpart. A small section of amp C on WFC2 in the difference image is shown in Figure 1. Pixels with high dark rates in the Daily Monitor superdark (>5 e^-/s) are marked with circles if they are stable and squares if they are unstable (DQ flag 32). Nearly all of the stable pixels are bright in the difference image, indicating that their dark rates are higher in the Pilot superdark than in the Daily Monitor superdark. Some of the unstable pixels are bright as well, but some are dim, as is expected for pixels with unstable dark rates.

3 Analysis of Fading Behavior

To further investigate these discrepant dark rates, we measured the dark rate in hot, stable pixels in all dark and external full-frame data from the Oct 2020 anneal period. The frames were bias-corrected, CTE-corrected, and if necessary, flash-corrected. Regions around highly saturated pixels in the Daily Monitor superdark, like those discussed in Cohen & Grogin (2020) and Cohen et al. (2020), were masked.

An estimate of the sky background was removed from each external frame in order to isolate the dark current of the hot pixels. To find the sky background, we masked sources,

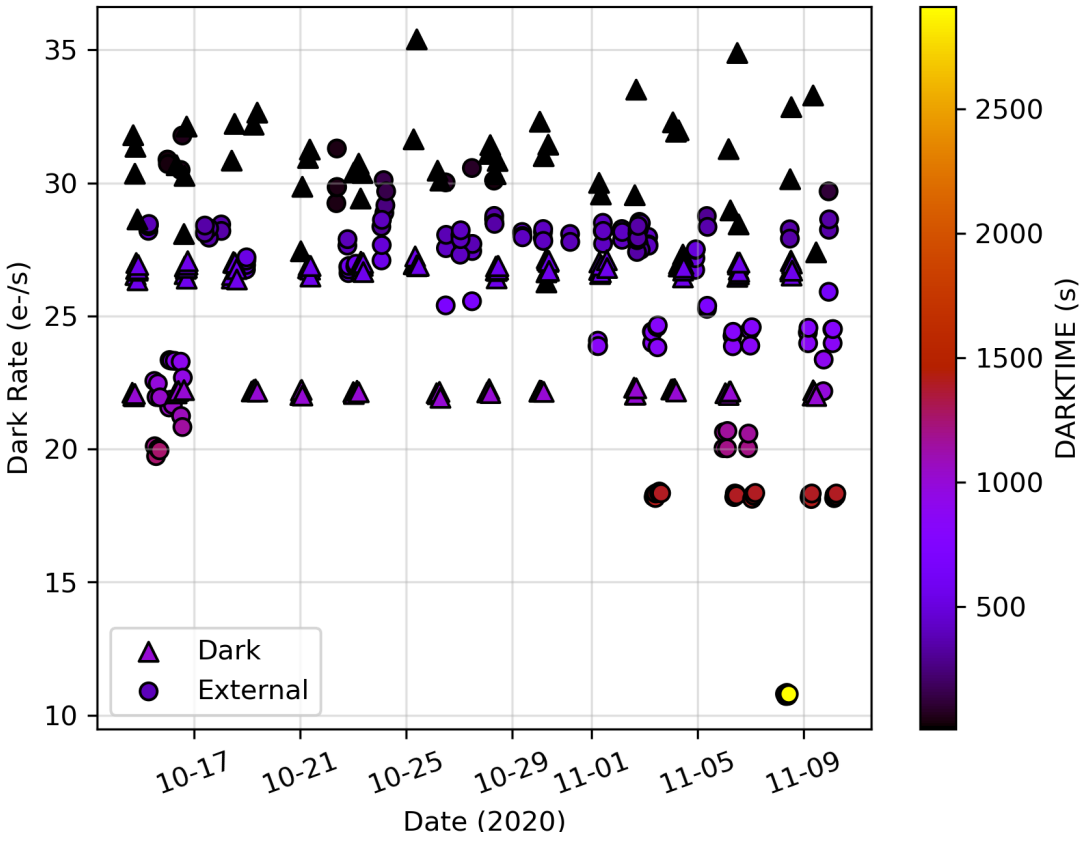

Figure 2: Dark rate as a function of observation date and time for every dark and external frame over the Oct 2020 anneal period for pixel (570, 174) on amp C. Two image types are plotted: external frames (circles) and dark frames (triangles). The DARKTIME of the frame determines the color of each point. A strong negative correlation between dark rate and DARKTIME for this pixel is clear.

cosmic rays, and CTE trails in the SCI arrays with `photutils.make_source_mask`[1] and calculated the 3σ-clipped median of the resulting masked arrays. The median dark current in the Daily Monitor superdark was estimated with the same steps and removed from the sky background.

Pixels flagged only as hot (DQ flag 16) with dark rates $\geq$5 e^-/s in the Daily Monitor superdark were selected from the masked, background-subtracted SCI arrays of each frame. The dark rate of each selected hot pixel was found by dividing the pixel value by the DARKTIME header keyword. DARKTIME is determined from timestamps in the Unique Data Log for each exposure, and is effectively the sum of exposure time (EXPTIME), flash duration (FLASHDUR), and a small amount of additional time, also called commanding overhead. In this report, we do not add a correction to DARKTIME for *additional* commanding overhead for either post-flashed or unflashed data because the fading trends are generally smoothest when an uncorrected DARKTIME is used to compute dark rates (see Ryon & Grogin (in

[1]We set nsigma = 2, npixels = 3, and dilate_size = 7.

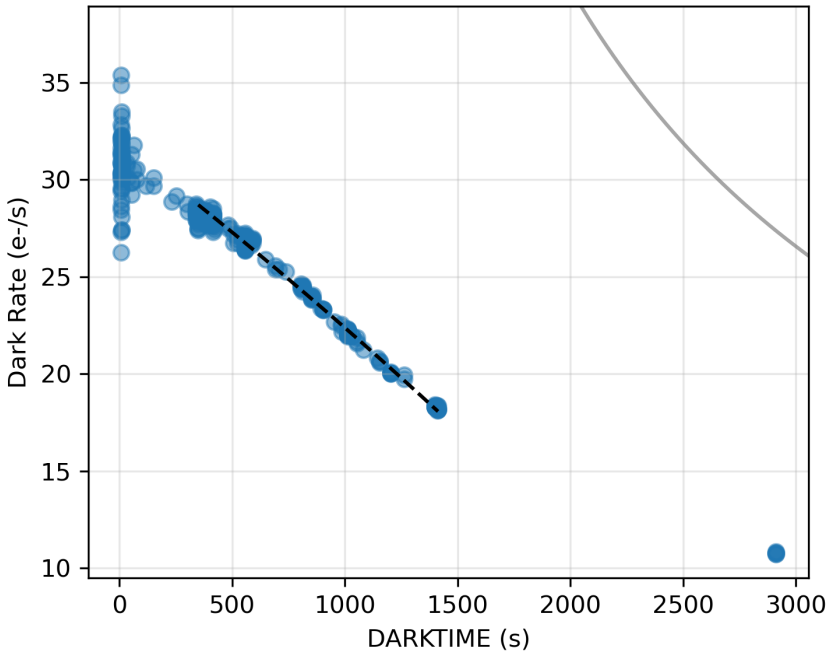

Figure 3: Dark rate as a function of DARKTIME for pixel (570, 174) in amp C from every dark and external frame in the Oct 2020 anneal period. The dashed black line shows a quadratic fit to data with 350s<DARKTIME<2000s. The solid gray line shows the saturation level for this pixel converted into dark rate.

prep) for more details).

In Figure 2, we plot dark rate as a function of observation date over the Oct 2020 anneal period for an example hot pixel located at (570, 174) on amp C. Outliers more than 5σ from the average dark rate were removed, as these are likely coincident with astronomical sources or cosmic rays. External frames are plotted as circles and dark frames are triangles. The color of each point represents the DARKTIME of the frame. This pixel is quite hot and stable at constant DARKTIME; ∼22 e-/s in the Daily Monitor dark frames over the course of the anneal period. There is a strong correlation between dark rate and DARKTIME, such that higher dark rates are found in shorter exposures and lower dark rates in longer exposures. In particular, this pixel's dark rate in the Pilot darks is nearly 5 e^-/s, or 20%, higher than in the Daily Monitor darks. We find no dependence on type of exposure, alleviating concerns that poor post-flash subtraction or another data processing error could be to blame.

In Figure 3, we plot dark rate directly as a function of DARKTIME for the same pixel as in Figure 2. Outliers more than 5σ from the average dark rate were again removed. The negative correlation between dark rate and DARKTIME is nearly linear and shows very little scatter over a large range in DARKTIME, particularly beyond ∼300s. The scatter at short DARKTIMEs is largely consistent with expected noise from dark current, post-flash (if present), and read noise, with the rest attributed to the pixel-based CTE correction. We call the overall behavior of this pixel "fading," although it is important to recall that each point represents the dark rate averaged over the exposure, not the instantaneous dark rate at a given moment during an exposure. The black dashed line is a 2nd-degree polynomial fit

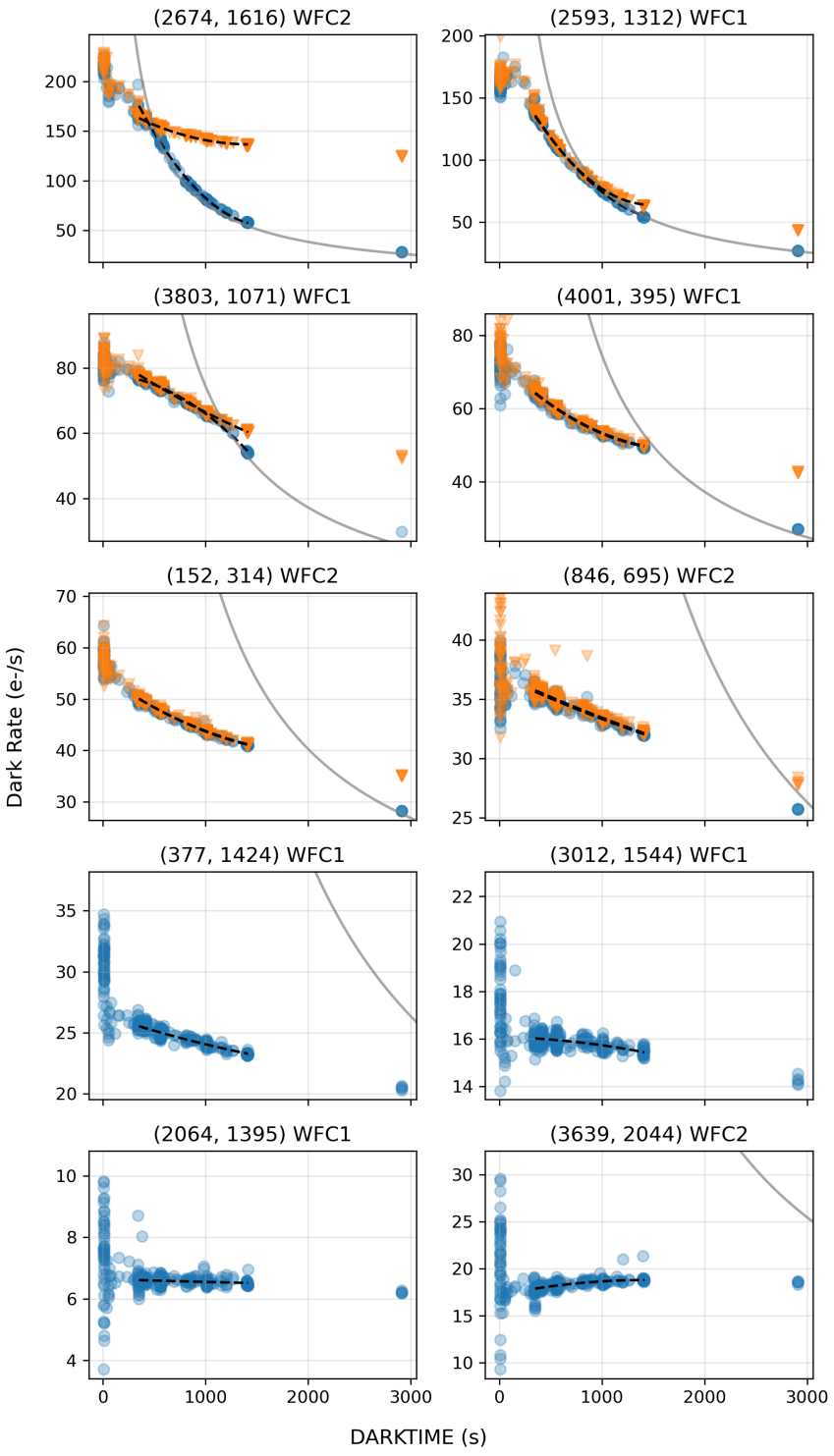

Figure 4: Same as Figure 3 for a representative sample of hot pixels spanning a range of dark rate and fading behavior. Pixels with dark rates >30 e^-/s in the Daily Monitor superdark have their total dark rate, including saturation overflow charge in adjacent pixels, plotted as orange triangles.

discussed further in Section 4. The solid gray line is the saturation threshold, taken from the saturation map from Cohen & Grogin (2020) and converted into dark rate over the relevant range of DARKTIMEs.

The fading behavior of ten more hot pixels is shown in Figure 4, roughly organized in order of decreasing dark current from top to bottom. Fading trends are typically linear or show a small amount of curvature beyond ∼300s. Below ∼300s, dark rates follow the trends less consistently, possibly because CTE losses are more difficult to reconstruct for pixels with fewer electrons (especially for those near the readout register). It is also evident that hotter pixels tend to fade more quickly than cooler pixels, which we explore more fully in Section 4. Interestingly, some pixels do show slight increases in dark rate as a function of DARKTIME, an example of which is shown in the bottom right panel.

The pixels in the top six panels saturate before DARKTIME∼3000s, as shown by the blue points intersecting and then following the saturation threshold towards increasing DARKTIME. Once a pixel saturates, the excess charge overflows into adjacent pixels along the column. To roughly reconstruct the total signal generated in these hot pixels after saturation, we sum the dark rates of hot pixels with dark rates ≥30 e^-/s (in the Daily Monitor superdark) together with their neighboring ±2 pixels in the column, which should contain most of the overflow charge. The total dark rates are plotted as orange triangles in Figure 4, and show that fading trends present prior to saturation persist beyond saturation.

4 Evolution with Time

To further assess the fading trends, we fit dark rates over 350s<DARKTIME<2000s with a 2nd-degree polynomial. The fits are represented by black dashed lines in Figures 3 and 4. Hot pixels in the rare full-orbit (∼3000s) exposure, a few of which appear in the Oct 2020 anneal period, sometimes depart from the overall trend. Since we are interested in studying fading behavior over typical exposure times and the vast majority of WFC exposures are <2000s, we do not include full-orbit frames in the fit.

The 2nd-degree polynomial describes most pixels' fading behavior and can be easily quantified into a "fading metric" for each pixel. We define this metric as the derivative of the fit at a representative DARKTIME of 1000s, or

$$\text{fading metric} = 2a \times \text{DARKTIME} + b = 2000a + b, \tag{1}$$

where a and b are the 2nd- and 1st-order coefficients of the fit, respectively. This metric is essentially the slope of the trend at the exposure time of the Daily Monitor dark frames with units of e^-/s/s. If the metric is negative, then the pixel generally fades as a function of exposure time, and if positive, then it generally brightens.

In Figure 5, we plot the fading metric as a function of dark rate in the Daily Monitor superdark. The black points are individual hot pixels from the Oct 2020 anneal period. For hot pixels with dark rates ≥30 e^-/s, the fading metric from the total dark rate, including saturation overflow, is plotted. There is a clear correlation between fading metric and dark rate, in that hotter pixels fade more quickly. The majority of hot pixels with dark rates <10-20 e^-/s display little to no fading, with fading metrics largely centering around zero. Above ∼20 e^-/s, the envelope of points widens and trends downward.

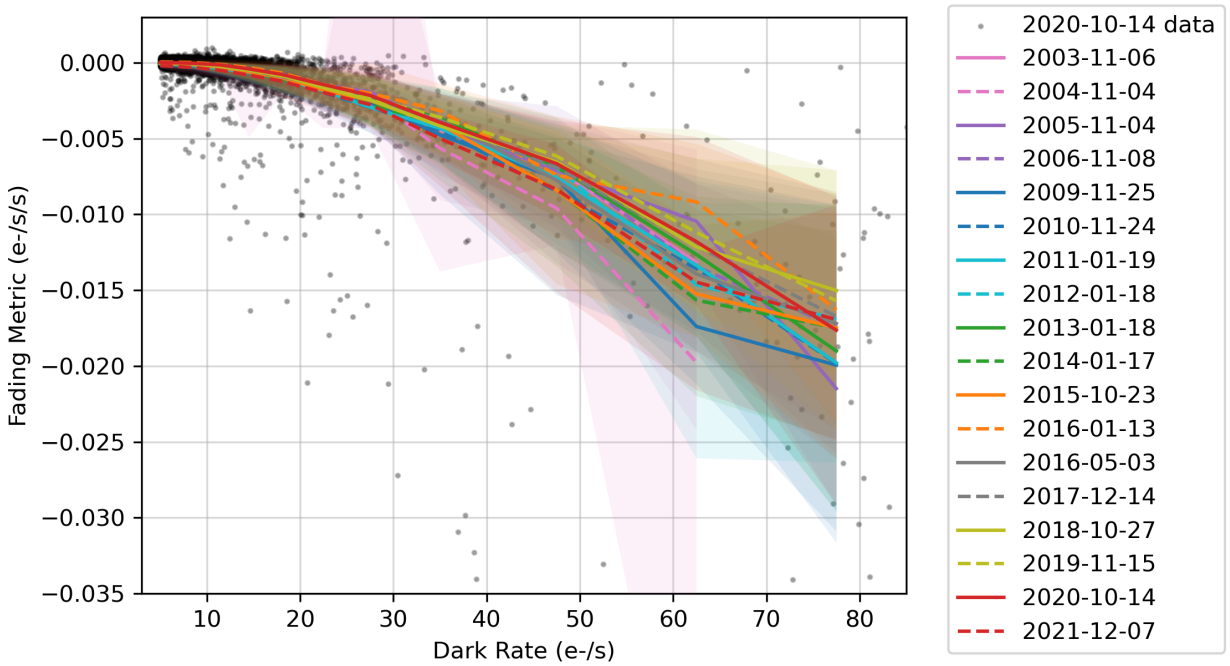

Figure 5: Fading metric as a function of dark rate in the Daily Monitor superdark. Black points represent individual hot pixels from the Oct 2020 anneal. Colored lines and shaded regions are median and $\pm 1\sigma$ fading metrics for several anneal periods.

We perform the same analysis on hot pixels from several additional anneal periods, about one per year over the lifetime of ACS. In Figure 5, the median and $\pm 1\sigma$ fading metrics in bins of dark rate are represented by colored solid and dashed lines and shaded regions for each anneal period. There are many fewer hot pixels in dark frames from early in ACS' lifetime (2003 and 2004), which causes the pink shaded regions to be noisier than the others. While there is a large amount of scatter in the median trends at high dark rates, no clear evolution of the fading metrics over time is seen. Therefore, fading hot pixels have been present and, as a population, have shown the same overall fading behavior since ACS was installed on HST.

5 Effect on Science Data & New DQ Flagging

During dark correction of WFC science frames by CALACS, all pixels are treated as if they accumulate dark current constantly with time. As a result, hot pixels with non-constant dark rates will not be accurately corrected unless the science frame is the same length as the superdark (1000s). The magnitude of under- or over-correction therefore depends on the difference in DARKTIME between the science frame and superdark.

For example, assume a 350s science frame populated with hot pixels affected by fading according to the Oct 2020 median fading metrics (red solid line in Figure 5). If we approximate the fading trends as linear with respect to DARKTIME for simplicity, then we can calculate the number of electrons remaining after dark correction. This remaining signal can also be expressed as a percentage of the hot pixel signal and compared to the expected

Table 1: Remaining Dark Signal in Median Fading Hot Pixels after Dark Correction of 350s Frame

Dark Rate (e^-/s)	**Remaining Dark Signal (e^-)**	**Percentage of Hot Pixel Signal (%)**	**Factors of Poisson Noise (×)**
5.0	-3.0	-0.2	-0.1
8.5	10.0	0.3	0.2
11.5	36.0	0.9	0.6
14.5	95.5	1.9	1.3
18.0	176	2.8	2.2
22.5	330	4.2	3.7
27.5	491	5.1	5.0
35.0	895	7.3	8.1
47.5	1515	9.1	12
62.5	2685	12	18
77.5	4012	15	24

Poisson noise of the hot pixel, all listed in Table 1.

Very hot pixels ($\gtrsim$20 e^-/s in superdarks) are quite poorly corrected, on average. Careful inspection of Figure 5 also shows that the $+1\sigma$ envelopes for all anneals fall below zero fading metric at $\sim$20 e^-/s, indicating that nearly all pixels above this dark rate are fading in every anneal studied. Fortunately, the number of hot pixels with dark rates $\gtrsim$20 e^-/s is small, $\lesssim$800 in most recent anneal periods, or 0.005% of the detector.

Despite their relative rarity, poorly-corrected hot pixels may impact photometry if the targets are faint and placed in unfortunate locations on the detectors. This is especially true if exposure times are significantly different than 1000s and if dithers are not used to sample "clean" regions of the detectors.

We therefore flag hot pixels with dark rates $\geq$20 e^-/s with DQ flag 32 in all superdarks, which is currently used for unstable pixels. The definition of DQ flag 32 has therefore been expanded to include any kind of pixel instability, including fading dark rates. During dark correction in CALACS, these flags will propagate into the DQ arrays of science data. Updated superdarks will be delivered to the Calibration Reference Data System (CRDS) shortly after the publication of this report.

Adjustment of hot pixel dark rates to correct for fading is possible, but would require significant data processing and resources to accomplish for every anneal period. Users are encouraged to contact the HST Help Desk[2] if interested in careful correction of hot pixels in their WFC data.

[2] `https://stsci.service-now.com/hst`

6 Discussion & Conclusions

In this work, we have characterized hot pixels in ACS/WFC that do not exhibit constants dark rates over the course of an exposure. The dark rates of most very hot pixels decline with increasing exposure time, often linearly or with slight curvature. Fading hot pixels are explained by declining field-assisted charge generation, which is due to electric fields weakening as charge is accumulated (Janesick, 2001). The fading behavior of individual hot pixels is due to the combination of the number of lattice defects and the local electric fields within the pixel (M. Sirianni priv. comm.).

We also find that hotter pixels tend to fade more quickly than cooler pixels. Charge accumulates more rapidly in hotter pixels, reducing electric field strength more quickly and leading to a faster dropoff in field-assisted charge generation (M. Sirianni priv. comm.). Additionally, the relationship between fading metric and dark rate has not appreciably changed over the lifetime of ACS. From this, we can conclude that radiation damage does not change the underlying operation of the detectors, rather, it simply results in more defects and more hot pixels.

Poor correction of hot pixels due to inconsistent dark rates between science frames and superdarks may affect certain science cases. To mitigate these effects, all hot pixels $\geq$20 e^-/s will henceforth be flagged in superdarks as unusable for science purposes. Users studying faint sources in existing data are encouraged to inspect their data for residual hot pixels.

Acknowledgements

The authors thank Marco Sirianni for enlightening discussions regarding CCD detector physics. The authors also thank the following ACS team members for taking the time to review and provide feedback on this report: Jay Anderson, Nimish Hathi, Gagandeep Anand, David Stark, Roberto Avila, and Yotam Cohen.

This work makes use of `jupyter` (Kluyver et al., 2016), `numpy` and `scipy` (Virtanen et al., 2019), `pandas` (McKinney, 2010), `astropy` (Astropy Collaboration et al., 2013; Price-Whelan et al., 2018), and `matplotlib` (Hunter, 2007).

References

Astropy Collaboration, Robitaille, T. P., Tollerud, E. J., et al. 2013, A&A, 558, A33

Borncamp, D., Grogin, N., Bourque, M., & Ogaz, S. 2017, Pixel History for Advanced Camera for Surveys Wide Field Channel, ACS ISR 2017-05, STScI

Cohen, Y., & Grogin, N. A. 2020, New and Improved Saturated Pixel Flagging for the ACS/WFC, ACS ISR 2020-02, STScI

Cohen, Y., Olaes, M. K., & Grogin, N. A. 2020, Unusual Horizontal Charge Overflow from Saturated CCD Pixels in the ACS WFC: Discovery and Remediation, ACS ISR 2020-07, STScI

Desjardins, T. D., Miles, N. D., Ryon, J. E., & Borncamp, D. 2018, ACS/WFC Superbias, Superdark, and Sink Pixel File Generation, ACS TIR 2018-01, STScI

Hunter, J. D. 2007, Computing in Science & Engineering, 9, 90

Janesick, J. R. 2001, Scientific charge-coupled devices (SPIE Press)

Jones, M. R. 2000, ACS WFC CCD Radiation Test: The Radiation Environment, ACS ISR 2000-09, STScI

Kluyver, T., Ragan-Kelley, B., Pérez, F., et al. 2016, in Positioning and Power in Academic Publishing: Players, Agents and Agendas, ed. F. Loizides & B. Schmidt, IOS Press, 87 – 90

McDonald, M. C., Desjardins, T. D., & Miles, N. D. 2020, Anneal Efficacy in the Advanced Camera for Surveys Wide Field Channel, ACS ISR 2020-05, STScI

McKinney, W. 2010, in Proceedings of the 9th Python in Science Conference, ed. S. van der Walt & J. Millman, 51 – 56

Ogaz, S., Anderson, J., & Golimowski, D. 2015, Post-Flash Calibration Darks for the Advanced Camera for Surveys Wide Field Channel (ACS/WFC), ACS ISR 2015-03, STScI

Price-Whelan, A. M., Sipőcz, B. M., Günther, H. M., et al. 2018, AJ, 156, 123

Ryon, J. E., et al. 2022, Advanced Camera for Surveys Instrument Handbook for Cycle 30 v.21.0 (Baltimore: STScI)

Ryon, J. E., & Grogin, N. A. in prep

Ryon, J. E., Grogin, N. A., & McDonald, M. C. 2021, An Exploration of Reduced Exposure Time and Post-Flash Duration of ACS/WFC Calibration Darks, ACS TIR 2021-01, STScI

Sirianni, M., Mutchler, M., & Lucas, R. A. 2006, in The 2005 HST Calibration Workshop: Hubble After the Transition to Two-Gyro Mode, ed. A. M. Koekemoer, P. Goudfrooij, & L. L. Dressel, 45

Virtanen, P., Gommers, R., Oliphant, T. E., et al. 2019, arXiv e-prints, arXiv:1907.10121